Submitted to ApJ, 17 Nov 2003

The Linear Instability of Astrophysical Flames in Magnetic Fields

L. J. Dursi[1]

ABSTRACT

Supernovae of Type Ia are used as standard candles for cosmological observations despite the as yet incomplete understanding of their explosion mechanism. In one model, these events are thought to result from subsonic burning in the core of an accreting Carbon/Oxygen white dwarf that is accelerated through flame wrinkling and flame instabilities. Many such white dwarfs have significant magnetic fields. Here we derive the linear effects of such magnetic fields on one flame instability, the well-known Landau-Darrieus instability. When the magnetic field is strong enough that the flame is everywhere sub-Alfvénic, the instability can be greatly suppressed. Super-Alfvénic flames are much less affected by the field, with flames propagating parallel to the field somewhat destabilized, and flames propagating perpendicular to the field somewhat stabilized. Trans-Alfvénic parallel flames, however, like trans-Alfvénic parallel shocks, are seen to be non-evolutionary; understanding the behavior of these flames will require careful numerical simulation.

Subject headings: supernovae: general — white dwarfs – hydrodynamics — MHD — nuclear reactions, nucleosynthesis, abundances — conduction

1. INTRODUCTION

1.1. Supernovae Type Ia Progenitors

The current standard model for Type Ia supernova explosions is that a flame or flames begin inside a Carbon-Oxygen Chandrasekhar mass white dwarf (see for instance the review by Hillebrandt and Niemeyer (2000)). The burning may accelerate by flame instabilities; the Carbon-Oxygen flame is unstable to the Landau-Darrieus and Rayleigh-Taylor instabilities (Bychkov and Liberman 1995) which wrinkles the flame front, burning a larger surface area of material per unit time.

Although the class of white dwarfs that forms the progenitors for Type Ia supernovae is unclear, it is known that many white dwarfs have significant surface magnetic fields, up to 10^8 G for accreting systems and isolated systems with magnetic fields up to 10^9 G are known; central magnetic fields may be much larger (see the review by Wickramasinghe and Ferrario 2000, and new data in for instance Schmidt et al. 2003). Fields of this strength may certainly affect the dynamics of flame instabilities, and thus the mechanism of supernovae. It is known that magnetic fields can destabilize shocks (see for example Stone and Edelman 1995 and references therein), and suppress other interfacial instabilities, such as Richtmeyer-Meshkov (Samtaney 2003) and Rayleigh-Taylor (Chandrasekhar 1981).

[1]Dept. of Astronomy & Astrophysics, The University of Chicago, Chicago, IL 60637

In terrestrial chemical combustion, many intermediate species are ionized, so that magnetic fields might be thought to have a dynamic effect. However, research on flames in magnetic fields has been sparse in the terrestrial flame literature because the diffusion of magnetic fields under in terrestrial burning conditions is fast enough that any interaction between the flame and the magnetic field is quite limited. Some recent work has been done on the effect of ambient magnetic fields on chemical flames (Mizutani et al. 2001; Wakayama and Sugie 1996) where small effects were found mainly due to the effect on large-scale motions of paramagnetic gases such as O_2.

In the astrophysical case magnetic fields may be more relevant, and the flame-field interactions may be richer in this extremely large magnetic Reynolds number regime, as perturbations in the magnetic field cannot readily diffuse away. Although there has been some look at large-scale burning dynamics in the presence of a large magnetic field (Ghezzi et al. 2001), little work has been presented on the microphysics of flame dynamics in the presence of a magnetic field.

In this paper, we present a linear-stability analysis of the hydrodynamic flame instability, or Landau-Darrieus instability (Landau 1944; Darrieus 1938) in the presence of a magnetic field.

1.2. Landau-Darrieus Instability

The physical scenario of the Landau-Darrieus instability is sketched in Fig.1, where burning proceeds in a subsonic wave (a deflagration wave, or a flame), propagating as a plane. For simplicity, we consider the frame of the unperturbed flame. The flame structure itself is not modelled here; instead, we consider the flame to be an infinitesimally thin interface propagating at a known speed, S_l, into the fuel. In the original Landau-Darrieus derivation, the flame speed was assumed to be so much slower than the sound speed that the unburned fuel and burned ash regions could be assumed to have incompressible flows; in our astrophysical case, this assumption also holds (Timmes and Woosley 1992). We use subscript b to refer to quantities in the burned region, and u to refer to quantities in the unburned region. Fuel approaches the flame with a velocity equal to S_l.

The reaction that drives the propagating flame is assumed to be exothermic enough that the density behind the flame, ρ_b is lower than the density ahead of the flame, ρ_u. This is expressed as a density ratio, $\alpha = \rho_u/\rho_b > 1$. In this case, streamlines are refracted by the density jump across the flames, so that any initial wrinkling of the flame drives further wrinkling (see for instance Williams 1985, and Fig. 2.) This instability, driven by the density jump and mediated by hydrodynamic waves, is the well-known Landau-Darrieus instability, and in the linear regime it has an exponential growth rate of (*e.g.*, Bychkov and Liberman 2000)

$$\frac{n}{kS_l} = \frac{\alpha}{\alpha+1}\left(\sqrt{-\frac{g}{kS_l^2}\frac{\alpha^2-1}{\alpha^2}+\frac{\alpha^2+\alpha-1}{\alpha}}-1\right), \tag{1}$$

where n is the growth rate, k is the wavenumber of the perturbation, and g is the gravitational acceleration. This instability is thought to play roles in terrestrial combustion (see for instance the references in Bychkov and Liberman 2000), astrophysical combustion (Hillebrandt and Niemeyer 2000), and inertial confinement fusion (Piriz and Portugues 2003), as well as at QCD and electroweak transition fronts (Kajantie 1994; Huet et al. 1993) with possible astrophysical application to strange stars (Benvenuto et al. 1990), polymerization fronts (Allali et al. 2001) and evaporation fronts such as of liquid metals (Lesin et al. 1993).

The wrinkling perturbs the pressure and velocities on either side of the flame. If the flame's speed into

the fuel is taken to be fixed at its planar value (the applicability of this assumption to astrophysical flames is considered in Dursi et al. 2003), the velocity at which the flame wrinkles is equal to the perturbed fluid velocities at the interface – *e.g.*, the flame is advected by the perturbed velocity.

This hydrodynamical Landau-Darrieus instability has been analytically examined in further detail in the astrophysical context (Bychkov and Liberman 1995; Blinnikov et al. 1995; Blinnikov and Sasorov 1996). In this work, we extend the derivation of the classical Landau-Darrieus instability to the case of the presence of a magnetic field. In §2, we consider a background magnetic field oriented along the direction of flame propagation. In §3, we consider a background magnetic field oriented transverse to the direction of propagation. In §4 we examine the self-consistency of assuming a fixed flame propagation speed when thermal diffusion will preferentially operate along magnetic field lines, In §5 we examine the effect of non-constancy of flame speed due to curvature, and we conclude in §6.

2. FIELD ALONG DIRECTION OF FLAME PROPAGATION

2.1. Perturbation equations

Here we derive the linear growth rate of the magnetic Landau-Darrieus instability. We follow closely the approach and notation of Chandrasekhar (1981). We begin with the equations of incompressible magnetohydrodynamics in an inviscid, perfectly conducting fluid:

$$\frac{\partial U_i}{\partial t} + U_j \frac{\partial U_i}{\partial x_j} - \frac{B_j}{4\pi\rho}\left(\frac{\partial B_i}{\partial x_j} - \frac{\partial B_j}{\partial x_i}\right) = -\frac{1}{\rho}\frac{\partial p}{\partial x_i} + g_i \frac{\delta\rho}{\rho} \tag{2}$$

$$\frac{\partial B_i}{\partial t} + \frac{\partial}{\partial x_j}\left(U_j B_i - B_j U_i\right) = 0 \tag{3}$$

$$\frac{\partial U_i}{\partial x_i} = 0 \tag{4}$$

$$\frac{\partial B_i}{\partial x_i} = 0 \tag{5}$$

where x_i is the i-coordinate, U_i is the velocity in the i-coordinate direction, ρ is density, $\delta\rho$ is any fluctuation in the density, p is pressure, B is the magnetic field, g is the gravitational acceleration, and summation over repeated indicies is implied. We assume constant density states ($\delta\rho = 0$) on the burned and unburned sides, with both gravity and a magnetic field pointing in the direction of propagation (which we take here to be $\vec{\mathbf{z}}$). We consider velocity, magnetic fields, and pressure of the form

$$\mathbf{U} = (u, v, w + W) \quad u, v, w \ll W, \tag{6}$$

$$\mathbf{B} = (b_x, b_y, b_z + B) \quad b_x, b_y, b_z \ll B, \tag{7}$$

$$p = P + \delta p \quad \delta p \ll P, \tag{8}$$

where P, B, and W are constant within each region. The velocity W_u with which the fuel approaches the flame is taken to be S_l, the flame speed, so that the unperturbed flame would be motionless. We will assume that all velocities are highly non-relativistic, so that displacement currents and relativistic effects may be neglected. We also assume that the flame and flow velocities are much less than the sound speed, and thus may consider incompressible flow. These assumptions are all appropriate for the slow flames in highly degenerate material that we consider here.

We then expand the MHD equations to linear order in the perturbed quantities, writing out explicitly the components of the vector equations. The linearization is described in more detail in Appendix A. We obtain:

$$\frac{\partial u}{\partial t} + W\frac{\partial u}{\partial z} - \frac{B}{4\pi\rho}\left(\frac{\partial b_x}{\partial z} - \frac{\partial b_z}{\partial x}\right) = -\frac{1}{\rho}\frac{\partial}{\partial x}\delta p \tag{9}$$

$$\frac{\partial v}{\partial t} + W\frac{\partial v}{\partial z} - \frac{B}{4\pi\rho}\left(\frac{\partial b_y}{\partial z} - \frac{\partial b_z}{\partial y}\right) = -\frac{1}{\rho}\frac{\partial}{\partial y}\delta p \tag{10}$$

$$\frac{\partial w}{\partial t} + W\frac{\partial w}{\partial z} = -\frac{1}{\rho}\frac{\partial}{\partial z}\delta p, \tag{11}$$

$$\frac{\partial b_x}{\partial t} + W\frac{\partial b_x}{\partial z} = B\frac{\partial u}{\partial z} \tag{12}$$

$$\frac{\partial b_y}{\partial t} + W\frac{\partial b_y}{\partial z} = B\frac{\partial v}{\partial z} \tag{13}$$

$$\frac{\partial b_z}{\partial t} + W\frac{\partial b_z}{\partial z} = B\frac{\partial w}{\partial z}, \tag{14}$$

$$\frac{\partial u}{\partial x} + \frac{\partial v}{\partial y} + \frac{\partial w}{\partial z} = 0 \tag{15}$$

$$\frac{\partial b_x}{\partial x} + \frac{\partial b_y}{\partial y} + \frac{\partial b_z}{\partial z} = 0. \tag{16}$$

We now consider normal modes, where all perturbed quantities have x, y, and t dependencies of the form $\exp(ik_x x + ik_y y + nt)$. In that case, and using D to denote d/dz, the equations become

$$(n + WD)\, u - \frac{B}{4\pi\rho}\left(Db_x - ik_x b_z\right) = -\frac{ik_x}{\rho}\delta p \tag{17}$$

$$(n + WD)\, v - \frac{B}{4\pi\rho}\left(Db_y - ik_y b_z\right) = -\frac{ik_y}{\rho}\delta p \tag{18}$$

$$(n + WD)\, w = -\frac{1}{\rho}D\delta p \tag{19}$$

$$(n + WD)\, b_x = BDu \tag{20}$$

$$(n + WD)\, b_y = BDv \tag{21}$$

$$(n + WD)\, b_z = BDw \tag{22}$$

$$Dw = -\left(ik_x u + ik_y v\right) \tag{23}$$

$$Db_z = -\left(ik_x b_x + ik_y b_y\right). \tag{24}$$

Adding $-ik_x$ times Eq. 17 to $-ik_y$ times Eq. 18 and using Eqs. 23 and 24 gives us

$$(n + WD)\, Dw - \frac{B}{4\pi\rho}(D^2 - k^2)b_z = -\frac{k^2}{\rho}\delta p. \tag{25}$$

Applying D again and substituting δp from Eq. 19 gives

$$(n + WD)\,(D^2 - k^2)w - \frac{B}{4\pi\rho}(D^2 - k^2)Db_z = 0. \tag{26}$$

Applying $(n + WD)$ to this and applying a component of the induction equation, Eq. 22 gives

$$\left((n + WD)^2 - (aD)^2\right)(D^2 - k^2)w = 0 \tag{27}$$

where $a^2 \equiv B^2/(4\pi\rho)$ is the square of the Alfvén speed. Similar equations for the other variables are:

$$\left((n + WD)^2 - (aD)^2\right)(D^2 - k^2)D\delta p = 0 \tag{28}$$

$$\left((n + WD)^2 - (aD)^2\right)(D^2 - k^2)(n + WD)\, b_z = 0. \tag{29}$$

We note that we are free to consider rotations around the $\vec{\mathbf{z}}$ axis such that k_y is zero and $k = k_x$. If we do so, then b_y and v decouple from the other quantities and we need not consider them further. Then $u = (i/k)Dw$ and $b_x = (i/k)Db_z$, completing our set of equations.

The z-dependence of our perturbed variables, then, must be of the form

$$C^{(s^-)}e^{kz} + C^{(s^+)}e^{-kz} + C^{(e)}e^{-\frac{n}{W}z} + C^{(A^+)}e^{-\frac{n}{W+a}z} + C^{(A^-)}e^{-\frac{n}{W-a}z}. \tag{30}$$

where the $C^{(i)}$ are constants within each of the burned and unburned regions, and represent the amplitudes of waves which travel along the $\hat{\mathbf{z}}$-direction with speeds $-n/k$, n/k, W, $W + a$, and $W - a$, respectively. Since the perturbed quantities are small (order ϵ, as per Appendix A), these $C^{(i)}$ must also be small (order ϵ) quantities.

In the case of flames propagating at the Alfvén speed $W = a$ in either the unburned or burned medium, the terms $((n + WD)^2 - (aD)^2)$ become $n(n + (a + W)D)$, and thus only a wave corresponding to $C^{(A^+)}$, and not $C^{(A^-)}$, exists in that region.

The unburned state will contain only waves that propagate from the flame to $-\infty$; *i.e.*, those with negative speed. Since W and a are positive, and we are only interested in modes with the real component of n positive, this leaves the first wave, and the fifth if the flame is slower than the Alfvén speed: $W_u < a_u$. The perturbations in the unburned state are then:

$$\delta p_u = -\frac{\rho_u(n + W_u k)^2}{k^2}C_u^{(s^-)}e^{kz} - \rho_u a_u^2 C_u^{(A^-)}e^{-\frac{n}{W_u - a_u}z} \tag{31}$$

$$b_{zu} = BC_u^{(s^-)}e^{kz} + BC_u^{(A^-)}e^{-\frac{n}{W_u - a_u}z} \tag{32}$$

$$w_u = \frac{(n + W_u k)}{k}C_u^{(s^-)}e^{kz} + a_u C_u^{(A^-)}e^{-\frac{n}{W_u - a_u}z} \tag{33}$$

$$b_{xu} = iBC_u^{(s^-)}e^{kz} - iB\frac{n}{k(W_u - a_u)}C_u^{(A^-)}e^{-\frac{n}{W_u - a_u}z} \tag{34}$$

$$u_u = i\frac{(n + W_u k)}{k}C_u^{(s^-)}e^{kz} - i\frac{a_u}{k}\frac{n}{W_u - a_u}C_u^{(A^-)}e^{-\frac{n}{W_u - a_u}z} \tag{35}$$

where these expressions were taken by choosing the parameters for b_{zu}, calculating w_u from the induction equation and then δp from the momentum equation, and then finding b_{xu} from b_{zu} using the divergence condition on the magnetic field and similarly using incompressibility to find u_u from w_u.

The same process can be repeated for the burned state. This gives us:

$$\delta p_b = -\frac{\rho_b(n - W_b k)^2}{k^2}C_b^{(s^+)}e^{-kz} - \rho_b a_b^2 C_b^{(A^+)}e^{-\frac{n}{W_b + a_b}z} - \rho_b a_b^2 C_b^{(A^-)}e^{-\frac{n}{W_b - a_b}z} \tag{36}$$

$$b_{zb} = BC_b^{(s^+)}e^{-kz} + BC_b^{(A^+)}e^{-\frac{n}{W_b + a_b}z} + BC_b^{(A^-)}e^{-\frac{n}{W_b - a_b}z} \tag{37}$$

$$w_b = -\frac{(n-W_b k)}{k} C_b^{(s^+)} e^{-kz} - a_b C_b^{(A^+)} e^{-\frac{n}{W_b+a_b}z} + a_b C_b^{(A^-)} e^{-\frac{n}{W_b-a_b}z} \quad (38)$$

$$b_{xb} = -iBC_b^{(s^+)} e^{-kz} - iB\frac{n}{k(W_b+a_b)} C_b^{(A^+)} e^{-\frac{n}{W_b+a_b}z} - iB\frac{n}{k(W_b-a_b)} C_b^{(A^-)} e^{-\frac{n}{W_b-a_b}z} \quad (39)$$

$$u_b = i\frac{(n-W_b k)}{k} C_b^{(s^+)} e^{-kz} + i\frac{a_b}{k}\frac{n}{W_b+a_b} C_b^{(A^+)} e^{-\frac{n}{W_b+a_b}z} - i\frac{a_b}{k}\frac{n}{W_b-a_b} C_b^{(A^-)} e^{-\frac{n}{W_b-a_b}z}. \quad (40)$$

Note the absence of $C^{(e)} e^{-(n/W)z}$ terms; for consistency between the momentum equation and the magnetic field divergence condition, $C^{(e)}$ must be zero.

2.2. Jump Conditions

Having derived the form of the perturbations in each region, we must provide the matching conditions at the flame, treated here as a discontinuity, to solve for the perturbations and their growth rate. Jump conditions in an inviscid, perfectly conducting magnetic fluid are (see for instance Shu (1992); Tidman and Krall (1971)):

$$[B_n] = 0 \quad (41)$$

$$[\rho U_n] = 0 \quad (42)$$

$$\rho U_n [\mathbf{U_t}] - \frac{B_n}{4\pi} [\mathbf{B_t}] = 0 \quad (43)$$

$$\rho U_n [U_n] + \left[p + \frac{B_t^2}{8\pi}\right] = g z_f [\rho] \quad (44)$$

$$[U_n \mathbf{B_t}] - B_n [\mathbf{U_t}] = 0, \quad (45)$$

where $[f]$ represents the jump in quantity f across the discontinuity, a subscript n refers to the component normal to the discontinuity, and subscript t refers to components tangential to the discontinuity.

The velocity normal to the discontinuity, U_n, must be the flame speed S_l, which is prescribed; here we are considering the fixed flame speed $S_l = W_u$. Since the interface is moving with respect to the far upstream fluid at $W + w_i$, where w_i is the w-velocity at the interface, the flame must be being advected — that is, wrinkled — with a velocity of $W + w_i - U_n = w_i$.

The directions tangential to the flame can be determined by taking the derivatives of the flame position z_f, *e.g.*$\partial z_f/\partial x$ and $\partial z_f/\partial y$. Because the flame position (in the unperturbed flame frame) is being wrinkled by the perturbed fluid velocity, and is itself a perturbed quantity $z_f \sim e^{ik_x x + ik_y y + nt}$, we can express z_f in terms of w_i:

$$\frac{\partial}{\partial t} z_f = w_i \quad (46)$$

$$z_f = \frac{w_i}{n}. \quad (47)$$

where $w_i = w(z_f)$. The difference between $w(z_f)$ and $w(0)$ is of second order of smallness, so we consider $w_i = w(0)$. This gives us the normal and two tangential directions, to linear order:

$$\hat{\mathbf{n}} = \left(-\frac{ik_x}{n} w_i, -\frac{ik_y}{n} w_i, 1\right) \quad (48)$$

$$\hat{\mathbf{t}}_\mathbf{1} = \left(1, 0, \frac{ik_x}{n} w_i\right) \quad (49)$$

$$\hat{\mathbf{t}}_{\mathbf{2}} = \left(0, 1, \frac{ik_y}{n} w_i\right). \tag{50}$$

We note again that we can ignore the y-component, and $\hat{\mathbf{t}}_{\mathbf{2}}$. Then we have

$$B_n = b_z + B \tag{51}$$
$$B_t = b_x + \frac{ik}{n} w_i B \tag{52}$$
$$U_t = u + \frac{ik}{n} w_i W \tag{53}$$
$$U_n = W. \tag{54}$$

To zeroth order in the perturbed quantities, then, the jump conditions are:

$$[B] = 0 \tag{55}$$
$$[\rho W] = 0 \tag{56}$$
$$\rho W\,[W] + [P] = 0 \tag{57}$$
$$\tag{58}$$

and linear order gives us

$$[b_z] = 0 \tag{59}$$
$$\rho W \left[u + \frac{ik}{n} w_i W\right] - \frac{B}{4\pi}\,[b_x] = 0 \tag{60}$$
$$[\delta p] = \frac{g w_i}{n}\,[\rho] \tag{61}$$
$$[W b_x] - B\,[u] = 0. \tag{62}$$

A further condition,

$$[w_i] = 0, \tag{63}$$

simply states that each side of the discontinuity travels with the same velocity.

The continuity of b_z across the interface implies (through the induction equation and the divergence-free property of the magnetic field) Eq. (62), so that Eq. (62) it may be discarded in favor of Eq. (59). This leaves us with four jump conditions: Eqns. (59), (60), (61), and (63).

We wish to solve for the perturbed quantities, so it is the linear-order jump conditions that we are interested in. The zeroth-order conditions give us some restrictions on the quantities (W, ρW, and B) that appear in the linear-order conditions.

We apply these conditions at $z = 0$, as z_f itself is a perturbed quantity, and as with w_i, the difference between applying the boundary conditions at $z = 0$ and $z = z_f$ will be of second order in smallness. Thus, for any jump condition $[f] = 0$, we set $f_b(0) - f_u(0) = 0$. These boundary conditions can then be expressed as a series of linear equations in the coefficients of the z dependences, $\mathcal{M} \cdot (C_u^{(s^-)}, C_b^{(s^+)}, C_b^{(A^+)}, C_u^{(A^-)}, C_b^{(A^-)})^T = 0$. The matrix $\mathcal{M}$ is

$$\begin{bmatrix} -(1+\bar{n}) & (\alpha-\bar{n}) & -\sqrt{\alpha}\,(\sqrt{\alpha}+\bar{a}_u) & 1-\bar{a}_u & \sqrt{\alpha}\bar{a}_u \\ -\left(1-\left(-2+\bar{a}_u^2\right)\bar{n}+\bar{n}^2\right) & \left(\alpha^2-2\alpha\bar{n}+\bar{n}\left(\bar{a}_u^2+\bar{n}\right)\right) & \frac{-(\sqrt{\alpha}+\bar{a}_u)\left(\alpha^2-\bar{n}^2\right)}{\sqrt{\alpha}} & (-1+\bar{a}_u)\left(-1+\bar{n}^2\right) & \frac{\bar{a}_u\left(\alpha^2-\bar{n}^2\right)}{\sqrt{\alpha}} \\ (1+\bar{n})\left(\bar{g}+\bar{n}+\bar{n}^2\right) & -\left(\frac{(\alpha-\bar{n})(\bar{g}+(\alpha-\bar{n})\bar{n})}{\alpha}\right) & -\left(\frac{(\sqrt{\alpha}+\bar{a}_u)(-\bar{g}+\sqrt{\alpha}\bar{a}_u\bar{n})}{\sqrt{\alpha}}\right) & (-1+\bar{a}_u)(\bar{g}+\bar{a}_u\bar{n}) & -\left(\frac{\bar{a}_u(\bar{g}+\sqrt{\alpha}\bar{a}_u\bar{n})}{\sqrt{\alpha}}\right) \\ -\bar{a}_u & \bar{a}_u & (\sqrt{\alpha}+\bar{a}_u) & -(-1+\bar{a}_u) & \bar{a}_u \end{bmatrix} \tag{64}$$

where $\bar{n} = n(kS_l)^{-1}$ is the dimensionless growth rate, $\bar{g} = g(kS_l^2)^{-1}$ is the dimensionless acceleration due to gravity, and $\bar{a}_u = a_u S_l^{-1}$ is the dimensionless Alfvén speed in the fuel. We have expressed all quantities in terms of the unburned state, using $\rho_u = \alpha\rho_b$, $S_l = W_u$, $\alpha W_u = W_b$, and $\sqrt{\alpha}a_u = a_b$.

2.3. Growth Rates

Depending on the relation of the flame and Alfvén velocities, different waves will be able to propagate away from the flame; this will determine the stability properties of the flame. The different regimes are shown in Fig. 3.

2.3.1. Super-Alfvénic flames: $W_u > a_u$; $W_b > a_b$

In this case, no Alfvén waves can travel upstream, so that $C_u^{(A^-)}$ must be zero. Then we have four constraints on four waves, and the system of equations represented by Eq. (64) has a solution if the determinant of $\mathcal{M}$ is zero;

$$\begin{aligned} &\left(\sqrt{\alpha}+\bar{a}_u\right)\left(-\alpha^2-\bar{n}^2+\alpha\left(\bar{a}_u^2+2\bar{n}\right)\right)\times \\ \left(\alpha^2\left(1+\bar{n}\right)+\left(1+\bar{n}\right)\left(\bar{g}-\bar{n}^2\right)-\alpha\left(1+\bar{g}+3\bar{n}-2\bar{a}_u^2\bar{n}+\bar{g}\bar{n}+3\bar{n}^2+\bar{n}^3\right)\right) &= 0 \end{aligned} \tag{65}$$

Further simplification, and the removal of two trivial solutions — $\bar{n} = \alpha \pm \sqrt{\alpha}\bar{a}_u$ — that lead to no actual wrinkling of the interface leaves us with:

$$\bar{n}^3 + \frac{1+3\alpha}{1+\alpha}\bar{n}^2 - \frac{\alpha^2+\alpha(2\bar{a}_u^2-\bar{g}-3)+\bar{g}}{1+\alpha}\bar{n} - \frac{\alpha^2-\alpha(\bar{g}+1)+\bar{g}}{1+\alpha} = 0. \tag{66}$$

In the limit of $\bar{a}_u \to 0$, this reproduces the well-known Landau-Darrieus result.

Absent gravity, we see that the constant term in the cubic is necessarily negative, so that a positive real solution always exists for $\bar{n}$ — that is, the interface is always unstable. The magnetic field cannot itself stabilize the flame in this case. One may examine the case of marginal stability in the presence of gravity by considering $\bar{n} = 0$. This requires $\alpha^2 - \alpha(\bar{g}+1) + \bar{g} = 0$. Since this does not include terms in $\bar{a}_u$, one must recover the Landau-Darrieus result; namely, that for stabilizing acceleration the condition of marginal stability is $\alpha = \bar{g}$, with larger α being unstable.

The maximum growth rate is plotted in this case for varying $\bar{g}$, α, and $\bar{a}_u$ in Fig. 4. We see that in this case, the instability is slightly enhanced over the non-magnetic ($\bar{a}_u = 0$) case.

2.3.2. 'Switch On' Alfvénic flames: $W_u = a_u$; $W_b > a_b$

When the upstream flow is exactly Alfvénic, a tangential field may "switch on" from zero in the upstream state to non-zero in the downstream state; such discontinuities are called "switch on" discontinuities (*e.g.*, Anderson 1963). If $W_u = a_u$, no $C_u^{(A^-)}$ wave exists, as in the strictly super-Alfvénic case, and all else remains the same; thus, the growth rate is the $\bar{a}_u \to 1$ limit of the super-Alfvénic case.

2.3.3. *Sub-Alfvénic flames: $W_u < a_u$; $W_b < a_b$*

In this case, upstream Alfvén waves may propagate, and thus $C_u^{(A^-)}$ may be non-zero but $C_b^{(A^-)}$ must be zero. Again, $\mathcal{M}$ becomes a square matrix and we may find the solution of the linear equations by calculating the determinant:

$$\begin{aligned}(-1+\bar{a}_u-\bar{n})\left(\alpha+\sqrt{\alpha}\bar{a}_u-\bar{n}\right)\Big(\alpha^{\frac{5}{2}}+\alpha^2\bar{n}-\bar{g}\bar{n}+\bar{n}^3-\sqrt{\alpha}\left(1+2\bar{a}_u\right)\left(\bar{g}-\bar{n}^2\right)-\\ \alpha^{\frac{3}{2}}\left(1+\bar{g}+2\left(2+\bar{a}_u\right)\bar{n}+\bar{n}^2\right)+\alpha\left(\bar{g}\left(2+2\bar{a}_u+\bar{n}\right)+\bar{n}\left(1+2\bar{a}_u^2+\bar{n}^2+2\bar{a}_u\left(1+\bar{n}\right)\right)\right)\Big) &= 0. \quad (67)\end{aligned}$$

Factoring out the two solutions ($\bar{n}=\bar{a}_u-1$, $\bar{n}=\sqrt{\alpha}\bar{a}_u+\alpha$) that result in trivial solutions, one again has a cubic in $\bar{n}$,

$$\begin{aligned}\bar{n}^3+\sqrt{\alpha}\frac{1-\alpha+2\bar{a}_u+2\sqrt{\alpha}\bar{a}_u}{1+\alpha}\bar{n}^2\\ +\frac{\alpha^2-2\alpha^{\frac{3}{2}}(2+\bar{a}_u)-\bar{g}+\alpha(1+2\bar{a}_u+2\bar{a}_u^2+\bar{g})}{1+\alpha}\bar{n}\\ +\frac{(\sqrt{\alpha}-1)\sqrt{\alpha}\left(\alpha+\alpha^{\frac{3}{2}}+\bar{g}(1+2\bar{a}_u-\sqrt{\alpha})\right)}{1+\alpha} &= 0. \quad (68)\end{aligned}$$

Note that in this case, even absent a gravitational acceleration g, the constant term in the cubic is positive, meaning that no positive real solution need exist.

If we express this in terms of n rather than $\bar{n}$, and take the limit $W_u \to 0$ (*e.g.*, the interface does not propagate into the fluid), one can reproduce the results of the Rayleigh-Taylor instability in the presence of a vertical magnetic field, as discussed in § 96 of Chandrasekhar (1981).

The scaled growth rate $\bar{n}$ as a function of α is shown in Fig. 5. The instability can be completely suppressed by the magnetic field. The region of stability is plotted in Fig. 6.

2.3.4. *'Switch Off' flames: $a_u > W_u$, $a_b = W_b$*

When the downstream flow is Alfvénic, a tangential field may "switch off" in the downstream case; such discontinuities are called "switch off" discontinuities.

If $W_b = a_b$, there can be no $C_b^{(A^-)}$ wave, and all proceeds as in the sub-Alfvénic case with $\bar{a}_u \to \sqrt{\alpha}$.

2.3.5. *Discussion*

Given that a sufficiently strong magnetic field suppresses the instability, it is somewhat surprising that while the flame is still super-Alfvénic, the growth rate of the instability actually increases with increasing magnetic field strength.

The reason for this is that the presence of a magnetic field allows for a non-zero jump in the tangential velocity across the flame, proportional to the jump in the tangential magnetic field component. From the jump conditions, we can calculate the ratio of the tangential magnetic fields across the interface as a function of $\bar{a}_u$; this is shown in Fig. 7. At the Alfvénic points, the flame becomes a 'switch on' or 'switch

off' discontinuity. For the super-Alfvénic flame ($\bar{a}_u < 1$), we see that the tangential magnetic field decreases across the flame, and thus so does the tangential velocity. In particular, in this case one has

$$\frac{U_{tb}}{U_{t_u}} = 1 - \frac{\alpha - 1}{\alpha - \bar{a}_u^2} \bar{a}_u^2 \frac{\bar{n} + 2}{(\bar{n} + 1)^2} \tag{69}$$

which is less than one. Since the magnitude of the tangential velocity decreases across the flame, the streamlines crossing the flame are bent still closer to the normal than in the purely hydrodynamical case shown in Fig. 2, and the instability is modestly enhanced.

2.3.6. Trans-Alfvénic flames: $W_u < a_u$; $W_b > a_b$

In this case the coefficients $C_b^{(A^+)}$, $C_u^{(A^-)}$, and $C_b^{(A^-)}$ may all be non-zero; we have a total of three Alfvén waves that may propagate to infinity from the flame front. Trans-Alfvénic flames then have more possible waves leaving the flame surface than boundary conditions to constrain them; there is no unique solution to the initial-value problem.

In this case, the discontinuity is said to be non-evolutionary (see for instance Anderson 1963, or a recent review by Markovskii and Somov 1996.) Analytically, these discontinuities have no solution to the semi-steady time evolution of a small perturbation; they must then undergo some finite-sized growth or change. In the case of an MHD shock, the consequences of nonevolutionarity are unclear; numerical simulations of MHD shocks have been seen to spontaneously break up into other discontinuities (Markovskii and Skorokhodov 2000), or stay relatively steady over long periods (Pogorelov and Matsuda 2000), depending on such things as shock geometry and strength. Numerical simulations will have to be performed to examine the behavior of flames in these circumstances.

Simply considering the dissipative structure of an MHD shock structure does not significantly reduce the range of parameters in which it is non-evolutionary(Markovskii and Somov 1996). It is possible that adding the physics of the (compressible) flame structure to the jump conditions as was done in Pelce and Clavin (1982) or Matalon and Matkowsky (1982) for terrestrial non-magnetic flames may select out a particular solution in this case. This has never been done with a magnetic field, and is well beyond the scope of this work.

It is possible, however, to constrain the possible evolution by parameterizing the allowed solutions. We consider taking the amplitude of the wave $C_u^{(A-)}$ as a free parameter; the algebra simplifies if one considers a scaled ratio of this wave to the other forward-going wave,

$$\theta = (\alpha - 1) \left[(\bar{a}_u - 1) \frac{C_u^{(A-)}}{C_u^{(s-)}} + 1 \right]. \tag{70}$$

Note that, depending on the phase difference between the waves, θ may be imaginary.

In this case, one obtains the following equation for the scaled growth rate,

$$\bar{n}^3 + \frac{4\alpha - \theta}{1 + \alpha} \bar{n}^2 - \frac{\alpha^2 - \alpha(\bar{g} - 2\bar{a}_u^2 + 3) + \bar{g}}{1 + \alpha} \bar{n} + \frac{\theta(\bar{g} - \alpha)}{1 + \alpha} = 0, \tag{71}$$

which reduces (as it must) to the superalfvénic relation if $C_u^{(A-)} = 0$.

One can investigate the effect of our free parameter θ on the growth rate, and one finds that the growth rate can be greatly enhanced, if $C^{(A-)}$ is very large compared to $C^{(s-)}$ and if they are in phase, or

almost stabilized if $C^{(A-)}$ is very large and exactly out of phase with $C^{(s-)}$; but unless there is a significant stabilizing gravitational acceleration, the flame remains unstable for the entire parameter range of solutions. A typical case is shown in Fig. 8, with $\bar{a}_u = 1.3$, $\bar{g} = 0$, and $\alpha = 2, 3, 4, 5$. Absent any selection criterion to select a unique θ, all that one can say is that the trans-alfvénic flames are unstable, with essentially arbitrary growth rate.

3. FIELD TRANSVERSE TO DIRECTION OF FLAME PROPAGATION

3.1. Perturbation equations

In the perpendicular-field case, the analysis is more straightforward as there is no competition between the flame velocity and the Alfvén velocity. We begin with Eqs. 2–4 from §2.1, but now our magnetic field is

$$\mathbf{B} = (b_x + B, b_y, b_z), \quad b_x, b_y, b_z \ll B. \tag{72}$$

In this case, our linearized equations in terms of normal modes are

$$\begin{aligned}
(n + WD)\, u &= -\frac{ik_x}{\rho}\delta p && (73)\\
(n + WD)\, v - \frac{B}{4\pi\rho}\left(ik_x b_y - ik_y b_x\right) &= -\frac{ik_y}{\rho}\delta p && (74)\\
(n + WD)\, w - \frac{B}{4\pi\rho}\left(ik_x b_z - D b_x\right) &= -\frac{1}{\rho} D\delta p && (75)\\
(n + WD)\, b_x &= ik_x B u && (76)\\
(n + WD)\, b_y &= ik_x B v && (77)\\
(n + WD)\, b_z &= ik_x B w && (78)\\
Dw &= -\left(ik_x u + ik_y v\right) && (79)\\
Db_z &= -\left(ik_x b_x + ik_y b_y\right). && (80)
\end{aligned}$$

Going through the same steps as in § 2, but working with b_x instead of b_z, we obtain:

$$\begin{aligned}
\left((n + WD)^2 + (ak_x)^2\right)(D^2 - k^2)u &= 0 && (81)\\
\left((n + WD)^2 + (ak_x)^2\right)(D^2 - k^2)\delta p &= 0 && (82)\\
\left((n + WD)^2 + (ak_x)^2\right)(D^2 - k^2)(n + WD)\, b_x &= 0. && (83)
\end{aligned}$$

Given the linearized equations, the perturbed quantities must have z-dependencies which are linear combinations of the following:

$$C^{(s^-)}e^{kz} + C^{(s^+)}e^{-kz} + C^{(e)}e^{-\frac{n}{W}z} + C^{(A^+)}e^{-\frac{n+iak_x}{W}z} + C^{(A^-)}e^{-\frac{n-iak_x}{W}z}. \tag{84}$$

We can then find the expressions for the perturbed quantities which satisfy the momentum and induction equations, and the divergence criterion for the velocity and magnetic field:

$$b_{xu} = B_u C_u^{(s^-)} e^{kz} \tag{85}$$

$$u_u = -i\frac{(n+W_u k)}{k_x}C_u^{(s^-)}e^{kz} \tag{86}$$

$$\delta p_u = \frac{\rho_u(n+W_u k)^2}{k_x^2}C_u^{(s^-)}e^{kz} \tag{87}$$

$$v_u = -i\frac{(n+W_u k)k_y}{k_x^2}C_u^{(s^-)}e^{kz} \tag{88}$$

$$w_u = -\frac{(n+W_u k)\left(1+\frac{k_y^2}{k_x^2}\right)}{k}C_u^{(s^-)}e^{kz} \tag{89}$$

$$b_{y_u} = B_u\frac{k_y}{k_x}C_u^{(s^-)}e^{kz} \tag{90}$$

$$b_{z_u} = -iB_u\frac{k}{k_x}C_u^{(s^-)}e^{kz} \tag{91}$$

$$b_{xb} = B_b C_b^{(s^+)}e^{-kz} + B_b C_b^{(A^+)}e^{-\frac{n+ia_b k_x}{W_b}z} + B_b C_b^{(A^-)}e^{-\frac{n-ia_b k_x}{W_b}z} \tag{92}$$

$$u_b = -\frac{i}{k_x}\left(n-W_b k\right)C_b^{(s^+)}e^{-kz} - a_b C_b^{(A^+)}e^{-\frac{n+ia_b k_x}{W_b}z} + a_b C_b^{(A^-)}e^{-\frac{n-ia_b k_x}{W_b}z} \tag{93}$$

$$\delta p_b = \rho_b\frac{(n-W_b k)^2}{k_x^2}C_b^{(s^+)}e^{-kz} - \left(\rho_b a_b^2\right)C_b^{(A^+)}e^{-\frac{n+ia_b k_x}{W_b}z} - \left(\rho_b a_b^2\right)C_b^{(A^-)}e^{-\frac{n-ia_b k_x}{W_b}z} \tag{94}$$

$$v_b = -ik_y\frac{n-W_b k}{k_x^2}C_b^{(s^+)}e^{-kz} - a_b C_b^{(A^+)'}e^{-\frac{n+ia_b k_x}{W_b}z} + a_b C_b^{(A^-)'}e^{-\frac{n-ia_b k_x}{W_b}z} \tag{95}$$

$$w_b = \frac{(n-W_b k)k}{k_x^2}C_b^{(s^+)}e^{-kz} - i\frac{W_b\left(k_x C_b^{(A^+)} + k_y C_b^{(A^+)'}\right)}{n+ia_b k_x}a_b e^{-\frac{n+ia_b k_x}{W_b}z} + i\frac{W_b\left(k_x C_b^{(A^-)} + k_y C_b^{(A^-)'}\right)}{n-ia_b k_x}a_b e^{-\frac{n-ia_b k_x}{W_b}z} \tag{96}$$

$$b_{y_b} = \frac{k_y}{k_x}B_b C_b^{(s^+)}e^{-kz} + B_b C_b^{(A^+)'}e^{-\frac{n+ia_b k_x}{W_b}z} + B_b C_b^{(A^-)'}e^{-\frac{n-ia_b k_x}{W_b}z} \tag{97}$$

$$b_{zb} = iB_b\frac{k}{k_x}C_b^{(s^+)}e^{-kz} + iW_b B_b\frac{k_x C_b^{(A^+)} + k_y C_b^{(A^+)'}}{n+ia_b k_x}e^{-\frac{n+ia_b k_x}{W_b}z} + iW_b B_b\frac{k_x C_b^{(A^-)} + k_y C_b^{(A^-)'}}{n-ia_b k_x}e^{-\frac{n-ia_b k_x}{W_b}z}. \tag{98}$$

As in § 2, $C_b^{(e)}$ must vanish.

3.2. Jump Conditions

The jump conditions will be the same as in §2.2, but the components of **B** will be different, and both tangential components must be considered since one is now selected by the direction of the magnetic field. We have

$$\mathbf{B_t} = (B+b_x, b_y) \tag{99}$$

$$B_n = b_z - \frac{ik_x}{n}wB \tag{100}$$

$$\mathbf{U_t} = \left(u + \frac{ik_x}{n} w_i W, v + \frac{ik_y}{n} w_i W\right) \quad (101)$$

$$U_n = W. \quad (102)$$

Then to zeroth order in the perturbed quantities, the jump conditions give us

$$[\rho W] = 0 \quad (103)$$

$$\rho W [W] + \left[P + \frac{B^2}{8\pi}\right] = 0 \quad (104)$$

$$[WB] = 0, \quad (105)$$

and to linear order,

$$\left[b_z - \frac{ik_x}{n} w_i B\right] = 0 \quad (106)$$

$$\rho W \left[u + \frac{ik_x}{n} w_i W\right] - \frac{1}{4\pi}\left(b_z - \frac{ik_x}{n} w_i B\right)[B] = 0 \quad (107)$$

$$\rho W \left[v + \frac{ik_y}{n} w_i W\right] = 0 \quad (108)$$

$$\left[\delta p + \frac{B b_x}{4\pi}\right] = \frac{g w_i}{n}[\rho] \quad (109)$$

$$[W b_x] = 0 \quad (110)$$

$$[W b_y] = 0. \quad (111)$$

3.3. Growth Rates

3.3.1. $k = k_y \hat{\mathbf{y}}$

Note that by Eqs. 81, 82, 83 the magnetic field only enters through ak_x, so that for $k_x = 0$ — that is, the perturbed mode is orthogonal to the magnetic field — these equations reduce to the equations for the Landau-Darrieus instability, and the magnetic field has no effect.

3.3.2. $k = k_x \hat{\mathbf{x}}$

In this case, as in § 2, again the $\hat{\mathbf{y}}$-components decouple, and we are left with only the linear equations for the $\hat{\mathbf{x}}$-components. The linearized equations have a non-zero solution only for

$$\begin{aligned} &- \left(\alpha^3 + \bar{a}_u^2 - 2\alpha^2 \bar{n} + \alpha \bar{n}^2\right) \\ \left(\alpha^3 (1+\bar{n}) - \bar{a}_u^2 (1+\bar{n}) - \alpha^2 (1+\bar{n}) \left(\bar{a}_u^2 + \bar{g} + (1+\bar{n})^2\right) + \alpha \left(2\bar{a}_u^2 + (1+\bar{n})\left(\bar{g} - \bar{n}^2\right)\right)\right) &= 0. \end{aligned} \quad (112)$$

Factoring out trivial solutions $\bar{n} = (\alpha \pm i\bar{a}_u \alpha^{-1/2})$ corresponding to no wrinkling of the interface, we are left with

$$\bar{n}^3 + \frac{1+3\alpha}{1+\alpha}\bar{n}^2 - \frac{\alpha^3 - \alpha^2(\bar{a}_u^2 + \bar{g} + 3) + \alpha\bar{g} - \bar{a}_u^2}{\alpha(\alpha+1)}\bar{n} - \frac{(\alpha-1)(\alpha^2 - \alpha(\bar{a}_u^2 + \bar{g}) + \bar{a}_u^2)}{\alpha(1+\alpha)} = 0 \quad (113)$$

In the limit of $\bar{a}_u \to 0$ this reduces to the correct Landau-Darrieus limit. Taking the other limit, in unscaled quantities, of $W_u \to 0$, one obtains

$$n^2 = gk\left(\frac{\rho_b - \rho_u}{\rho_b + \rho_u} - \frac{B_u^2 k^2\left(1+\alpha^2\right)}{4\pi g k^3\left(\rho_b + \rho_u\right)}\right). \tag{114}$$

Note that the second term in this expression is different than the result quoted in Chandrasekhar (1981) § 97, where it is assumed that the horizontal field is equal in both regions of the domain, and so we have here $B_u^2(1+\alpha^2) = B_u^2 + B_b^2$ rather than $2B^2$. If one repeats the derivation provided therein with $\alpha B_b = B_u$, as we have here, then the two results agree.

The maximum real solution of Eq. (113) is plotted in Fig. 9. We see that for $\bar{a}_u > 1$ there is significant suppression of growth of the instability, One can examine the stability boundary by considering $\bar{n} = 0$ in Eq. (113). This gives us

$$\alpha^2 - (\bar{a}_u^2 + \bar{g})\alpha + \bar{a}_u^2 = 0. \tag{115}$$

The minimum α for instability as a function of $\bar{a}_u$, for varying $\bar{g}$, is plotted in Fig. 10. Since a typical value for α for a carbon flame in a degenerate white dwarf is $\approx 1.3 - 2.4$ (*e.g.*, Dursi et al. 2003), one sees that once $\bar{a}_u$ exceeds 1, flame instability is greatly suppressed.

It should be noted here that the density ratio α, which in the non-magnetic case or in the case of § 2 is given by the physicochemical properties of the burning and the EOS of the fluid, here is also in principle a function of the magnetic field, as the ambient field also provides pressure support. However, in the limit where the sound speed is much larger than the Alfvén speed, this contribution is small.

4. LOCAL EFFECTS OF MAGNETIC FIELD ON FLAME VELOCITY

Astrophysical flames propagate by thermal diffusion. In the deep interior of a white dwarf, thermal diffusion is due largely to electrons; in the presence of a magnetic field, this diffusion will be anisotropic. (In outer regions of the star, where thermal diffusion is due to photons, there will be no such effect.) One must then investigate the range of validity of the assumption used in § 2 and § 3 that there will be a constant flame speed despite the wrinkling (and thus differing orientations) of the flame.

We will consider here a very simple model for the anisotropic thermal diffusion,

$$D_{\rm th}(\theta) = D_{\rm th}(0)\frac{a + b|\cos\theta|}{a+b} \tag{116}$$

where $D_{\rm th}$ is the thermal diffusivity, θ represents the angle between the direction of diffusion — that is, the local direction of flame propagation — and the ambient magnetic field, and a and b parameterize the anisotropy.

The local flame normal, from § 2 (but not restricted to linear order) is given by

$$\hat{\mathbf{n}} = \left(\frac{\partial}{\partial x} z_f, \sqrt{1 - \left(\frac{\partial}{\partial x} z_f\right)^2}\right) = \left(-\epsilon, \sqrt{1-\epsilon^2}\right). \tag{117}$$

Simple expressions for flame velocity (*e.g.*, Zeldovich and Frank-Kamenetskii 1938) find that the propagation velocity scales with the square root of the diffusivity. Thus, we will consider the angle dependence

of the flame velocity

$$S_l(\theta) = S_l(0)\sqrt{\frac{D_{\rm th}(\theta)}{D_{\rm th}(0)}} = S_l(0)\sqrt{\frac{a+b|\cos\theta|}{a+b}}. \tag{118}$$

4.1. Field parallel to flame propagation

In the case of the ambient magnetic field parallel to the direction of flame propagation discussed in § 2, with $\mathbf{B} = B\hat{\mathbf{z}}$. We then find

$$\cos\theta = \hat{\mathbf{B}}\cdot\hat{\mathbf{n}} = \sqrt{1-k^2z_f^2} = \sqrt{1-\epsilon^2}, \tag{119}$$

where $z_f k = \epsilon \ll 1$ as in Appendix A.

If we then expand our expression for $S_l(\theta)$ in terms of the small quantity kz_f one finds

$$\frac{S_l(\theta)}{S_l(0)} = 1 - \frac{b}{4\,(a+b)}\epsilon^2 + O\left(\epsilon^4\right), \tag{120}$$

that is, there is no correction to the flame speed to the linear order of the analysis we have performed in § 2. Thus, it is reasonable to consider a constant flame velocity in this case, at least for the simple angular dependence considered here.

4.2. Field perpendicular to flame propagation

On the other hand, for the case of the flame propagating across the magnetic field considered in § 3, $\mathbf{B} = B\hat{\mathbf{x}}$. In this case, $\cos\theta = \hat{\mathbf{B}}\cdot\hat{\mathbf{n}} = \hat{\mathbf{x}}\cdot\hat{\mathbf{n}} = -\epsilon$ which is of linear order, not quadratic order, in small quantities. In this case, we find

$$\frac{S_l(\theta)}{S_l(\pi/2)} = 1 + \frac{b}{2a}\epsilon + O\left(\epsilon^2\right) \tag{121}$$

so that for consistency to linear order, in this case the thermal diffusion must be nearly isotropic ($a \gg b$ — in particular, b/a must be of order ϵ). Note that for a perpendicular field, there would have to be a significant isotropic component to the diffusion anyway for there to be a meaningful propagating flame, since the flame must propagate by diffusion across the magnetic field; however, this is a weaker condition than $b/a \sim \epsilon$. Note that for diffusivities which depend more strongly on θ, such as $\cos^2(\theta)$, the flame speed will no longer depend on linear orders of perturbed quantities even for the perpendicular field.

5. EFFECTS OF CURVATURE

Independent of the effects of a magnetic field, it is well known that the velocity of a laminar flame depends on the details of the flame structure, and that curvature of the flame will change the flame speed. A simple relation for the modified flame speed was first given by Markstein (1964),

$$S_l = S_l^0\left(1 + l_M\frac{\partial^2 z_f}{\partial x^2}\right) \tag{122}$$

where S_l^0 is the planar flame speed, S_l is the modified flame speed, and l_M is an empirically determined 'Markstein length', which is divided by the radius of curvature of the flame. This simple prescription has

proved very robust, and Markstein lengths for some relevant astrophysical flames were numerically measured in Dursi et al. (2003).

This non-constancy of the flame speed can be incorporated into the results of §2 and §3. One first observes that in the unperturbed frame, the flame now moves with a velocity

$$W + w_i - S_l = w_i + k^2 z_f l_M W \quad , \tag{123}$$

and thus the perturbed flame position z_f is now

$$\begin{aligned} n z_f &= w_i + k^2 z_f l_M W & (124)\\ z_f &= \frac{w_i}{n - k^2 l_M W}. & (125) \end{aligned}$$

Because the flame position must be the same in both regions of the flame, the jump condition Eq. (63) becomes

$$[w_i] + k^2 z_f l_M [W] = 0. \tag{126}$$

In the case of the magnetic field parallel to the direction of propagation of the flame, jump conditions implicitly involving z_f must be modified appropriately to use Eq. (125), and Eq. (61) has a new term directly from the modified flame speed. The jump conditions become

$$\begin{aligned} [b_z] &= 0 & (127)\\ \rho W [u + ikz_f W] - \frac{B}{4\pi}[b_x] &= 0 & (128)\\ [\delta p] - 2k^2 z_f l_M \rho W [W] &= g z_f [\rho] & (129)\\ [W b_x] - B[u] &= 0. & (130) \end{aligned}$$

Again, the final jump condition may be discarded.

One can apply these boundary conditions and find the solution of the linear equations as in §2. For super-Alfvénic flames, one obtains for the growth rate

$$\begin{aligned} \bar{n}^3 + \frac{(1+3\alpha) - 2\alpha\bar{l}_M}{1+\alpha}\bar{n}^2 - \frac{\left(\alpha^2 + \alpha\left(2\bar{a}_u^2 - \bar{g} - 3\right) + \bar{g}\right) + 2\alpha(\alpha+1)\bar{l}_M}{1+\alpha}\bar{n} \\ - \frac{(\alpha-1)(\alpha-\bar{g}) + 2\alpha\bar{l}_M\left(\alpha - \bar{a}_u^2\right)}{1+\alpha} = 0, \end{aligned} \tag{131}$$

where $\bar{l}_M = k l_M$ is the non-dimensionalized Markstein length. Note that the above expression reduces to Eq. (66) for $\bar{l}_M \to 0$.

We can see how the Markstein length effects the growth rate in Fig. 11. If the Markstein length is comparable to the wavelength of the perturbation ($k l_M \approx 1$), the instability is greatly suppressed.

Since the effect for other cases is similar, we don't show growth rate plots, but for completeness, we include the expressions for growth rate here. For sub-Alfvénic flames, using the same jump conditions one obtains

$$\begin{aligned} \bar{n}^3 - \frac{\alpha^{\frac{3}{2}} - \sqrt{\alpha}(1 + 2\bar{a}_u) - 2\alpha\bar{a}_u + 2\alpha\bar{l}_M}{1+\alpha}\bar{n}^2 \\ \frac{\alpha^2 - 2\alpha^{\frac{3}{2}}(2 + \bar{a}_u) - \bar{g} + \alpha\left(1 + 2\bar{a}_u + 2\bar{a}_u^2 + \bar{g}\right)}{1+\alpha}\bar{n} - \bar{l}_M \frac{2\alpha\bar{a}_u(1+\sqrt{\alpha})}{1+\alpha}\bar{n} \end{aligned}$$

$$\frac{(-1+\sqrt{\alpha})\sqrt{\alpha}\left(\alpha+\alpha^{\frac{3}{2}}+\bar{g}-\sqrt{\alpha}\bar{g}+2\bar{a}_u\bar{g}\right)}{1+\alpha}+ \bar{l}_M\frac{2\alpha^{3/2}\left(1+\bar{a}_u-\bar{a}_u^2-\sqrt{\alpha}\left(1+\bar{a}_u\right)+\alpha\right)}{1+\alpha} = 0. \quad (132)$$

Trans-Alfvénic flames remain non-evolutionary, but again parameterizing the range of possible solutions one obtains

$$\bar{n}^3+\frac{(4\alpha-\theta)-2\alpha\bar{l}_M}{1+\alpha}\bar{n}^2 -\frac{\left(\alpha^2+\alpha\left(\bar{a}_u^2-\bar{g}-3\right)+\bar{g}\right)+2\alpha\left(1+\alpha\right)\bar{l}_M}{1+\alpha}\bar{n} +\frac{\theta(\bar{g}-\alpha)+2\alpha\bar{l}_M\left(\bar{a}_u^2-\theta-1\right)}{1+\alpha} = 0 \quad (133)$$

In the case of a magnetic field parallel to the flame, as in §3, the jump conditions become

$$[b_z-ik_xz_fB] = 0 \quad (134)$$

$$\rho W\left[u+ik_xz_fW\right]-\frac{1}{4\pi}\left(b_z-ik_xz_fB\right)[B] = 0 \quad (135)$$

$$\rho W\left[v+ik_yz_fW\right] = 0 \quad (136)$$

$$\left[\delta p+\frac{Bb_x}{4\pi}\right]-2k^2z_fl_M\rho W\left[W\right] = gz_f\left[\rho\right] \quad (137)$$

$$[Wb_x] = 0 \quad (138)$$

$$[Wb_y] = 0. \quad (139)$$

The modified expression for growth rate then becomes

$$\bar{n}^3+\frac{1+3\alpha-2\alpha\bar{l}_M}{1+\alpha}\bar{n}^2+\frac{-\alpha^3+\alpha^2\left(3+\bar{a}_u^2+\bar{g}\right)-\alpha\bar{g}+\bar{a}_u^2-2\bar{l}_M\alpha^2\left(\alpha+1\right)}{\alpha\left(1+\alpha\right)}\bar{n} -\frac{\left(\alpha-1\right)\left(\alpha^2-\alpha\left(\bar{a}_u^2+\bar{g}^2\right)+\bar{a}_u^2\right)+2\alpha\bar{l}_M\left(\alpha^2+\bar{a}_u^2\right)}{\alpha\left(1+\alpha\right)} = 0. \quad (140)$$

6. CONCLUSIONS

We have examined the growth of a small perturbation to a flame in ideal MHD, and compared the growth to the well-known results in the absence of a field. We find that for the magnetic field to greatly suppress the flame instability requires $a_u > W_u$. This requires extremely strong magnetic fields. Assuming some of the largest-observed magnetic fields in white dwarfs, we have

$$a_u \sim 3\times10^4 \text{ cm s}^{-1}\left(\frac{B}{10^9G}\right)\left(\frac{\rho}{10^8 \text{ g cm}^{-3}}\right)^{-1/2}. \quad (141)$$

With carbon-oxygen flame speeds in the core of a white dwarf more on the order of 10^6 cm s^{-1} (Timmes and Woosley 1992), this is likely too low to play a major in the entire star. However, localized strong magnetic field regions could easily have an effect; and it is known (Cattaneo 1999) that in chaotic flows such as the

turbulence that is likely to exist in a rotating white dwarf that even with originally extremely weak magnetic fields, local peaks are quickly generated with $\bar{a}_u \approx 1$.

On the surface of a neutron star, where the magnetic field might be the same but densities would be lower,

$$a_u \sim 1 \times 10^6 \text{ cm s}^{-1} \left(\frac{B}{10^9 G}\right) \left(\frac{\rho}{10^5 \text{ g cm}^{-3}}\right)^{-1/2}, \tag{142}$$

and magnetic field effects might well be significant everywhere.

Weaker magnetic fields also effect flame growth, but only modestly. If the flame is everywhere super-Alfvénic, the effects of magnetic field will somewhat stabilize the flame if the magnetic field is perpendicular to the flame propagation, and destabilize it if it is parallel.

It is instructive to compare the results presented here with those known for MHD shocks, where fast parallel shocks (which are super-Alfvénic) and perpendicular shocks are stable under a broad range of parameters (Gardner and Kruskal 1964), while slow shocks (which are sub-Alfvénic) are broadly unstable (Lesson and Deshpande 1967; Édel'man 1990; Stone and Edelman 1995); this is just the opposite of what is reported here. The key difference between the two, for the purposes of this instability, is the direction of the density jump across the discontinuity — recall that it is this density jump which drives the instability.

In the flames discussed here, heating from the reactions ensures that $\rho_b < \rho_u$; that is, $\alpha > 1$. However, in the case of a shock, in our notation $\alpha < 1$. This changes the underlying driving of the instability; indeed, if one uses $\alpha < 1$ in the growth rates presented above, one finds super-Alfvénic and parallel flames to be stable, and sub-Alfvénic flames to be unstable.

This difference also changes the properties of the nonevolutionary nature of the interface in the trans-Alfvénic case. In the case of a trans-Alfvénic MHD shock, there is one too few Alfvén waves to satisfy the boundary conditions, so there is no solution; in the case of a trans-Alfvénic flame, there is one too many, so there are an infinite number of solutions, and no unique solution. This will change the nature of the behavior in this regime. Future work must include numerical simulations of the interesting trans-Alfvénic flame regime, which could occur locally in a white dwarf and in large regions on the surface of a neutron star.

This work was supported by the Department of Energy Computational Science Graduate Fellowship Program of the Office of Scientific Computing and Office of Defense Programs in the Department of Energy under contract DE-FG02-97ER25308. The author thanks R. Rosner, A. Calder, and T. Dupont for helpful comments, and R. Morgan-Dursi for her support.

A. Linearization

A.1. MHD equations

In this section, we describe in more detail our process of linearizing the ideal MHD equations.

We perturb the initially planar flame with a very small amplitude wrinkle, giving it an initial perturbed position z_f. We require the amplitude to be small compared to the wavelength of the perturbation:

$$\frac{2\pi z_f}{\lambda} = z_f k = \epsilon \ll 1. \tag{A1}$$

Such a perturbation will generate perturbations in the magnetic fields and velocities of the same order; we expand them in series of this perturbation parameter ϵ. In the case of a parallel magnetic field,

$$\mathbf{B} = B\left(\epsilon b_{x1} + \epsilon^2 b_{x2} + \cdots, \epsilon b_{y1} + \epsilon^2 b_{y2} + \cdots, 1 + \epsilon b_{z1} + \epsilon^2 b_{z2} + \cdots\right) \tag{A2}$$

$$\mathbf{U} = W\left(\epsilon u_1 + \epsilon^2 u_2 + \cdots, \epsilon v_1 + \epsilon^2 v_2 + \cdots, 1 + \epsilon w_1 + \epsilon^2 w_2 + \cdots\right). \tag{A3}$$

Because the flow is incompressible, the pressure fluctuations will be fluctuations in the dynamic, not thermodynamic, pressure; thus the pressure fluctuations scale with ρW^2 rather than P:

$$p = P + \rho W^2 \epsilon \delta p_1 + \rho W^2 \epsilon^2 \delta p_2 + \cdots. \tag{A4}$$

We assume that all the non-dimensional expansion coefficients are of order unity. We will also assume that the non-dimensional parameters of the problem — the scaled growth rate ($\bar{n} = n/(kW)$), gravity ($\bar{g} = g/(kW^2)$) and Alfvén speed ($\bar{a}_u = a_u/W_u$) — are order unity quantities.

We may now write the ideal MHD equations in terms of these expansions. W, B, and ϵ are independent of time or position, and we retain terms up to first order in ϵ. For the momentum equation, we then have:

$$\epsilon\frac{\partial u_1}{\partial t} + W\epsilon\frac{\partial u_1}{\partial z} - \frac{B^2\epsilon}{4\pi\rho W}\left(\frac{\partial b_{x1}}{\partial z} - \frac{\partial b_{z1}}{\partial x}\right) = -W\epsilon\frac{\partial \delta p_1}{\partial x} \tag{A5}$$

$$\epsilon\frac{\partial v_1}{\partial t} + W\epsilon\frac{\partial v_1}{\partial z} - \frac{B^2\epsilon}{4\pi\rho W}\left(\frac{\partial b_{y1}}{\partial z} - \frac{\partial b_{z1}}{\partial y}\right) = -W\epsilon\frac{\partial \delta p_1}{\partial y} \tag{A6}$$

$$\epsilon\frac{\partial w_1}{\partial t} + W\epsilon\frac{\partial w_1}{\partial z} = -W\epsilon\frac{\partial \delta p_1}{\partial z}. \tag{A7}$$

Re-expressing the linear-order perturbed quantities in dimensional units, *e.g.* $(u, v, w) = \epsilon W(u_1, v_1, w_1)$, $(b_x, b_y, b_z) = \epsilon B(b_{x1}, b_{y1}, b_{z1})$, $\delta p = \epsilon\rho W^2 \delta p_1$, we obtain Eqns. (9–11). Other equations, and the boundary conditions, are linearized in the same manner.

A.2. Matching Boundary Conditions

In applying the boundary conditions at $z = z_f$, we can consider expanding the exponential z-dependencies in Taylor series. In the case of the magnetic field, expanding the exponential terms on the unburned side (the terms on the burned side are analogous) one obtains:

$$e^{-kz_f} = 1 - \epsilon + \epsilon^2 + \cdots \tag{A8}$$

$$e^{-\frac{n}{W_u + a_u}z_f} = 1 - \frac{\bar{n}}{1+\bar{a}_u}\epsilon + \frac{\bar{n}^2}{(1+\bar{a}_u)^2}\epsilon^2 + \cdots \tag{A9}$$

$$e^{-\frac{n}{W_u - a_u}z_f} = 1 - \frac{\bar{n}}{1-\bar{a}_u}\epsilon + \frac{\bar{n}^2}{(1-\bar{a}_u)^2}\epsilon^2 + \cdots, \tag{A10}$$

while the values for at $z = 0$ would clearly be exactly unity. Since these terms multiply the already order-ϵ coefficients $C^{(i)}$, then, the difference in the perturbed quantities between their values at $z = 0$ and $z = z_f$ is of order ϵ^2 and can be neglected in this analysis as long as $1 - \bar{a}_u \not\approx \epsilon$. As we will see, however, as $\bar{a}_u \to 1$, the terms of the form (A10) vanish, removing this restriction, and we may consider $z_f = 0$ for the boundary conditions.

REFERENCES

K. Allali, V. Volpert, and J. A. Pojman. Influence of vibrations on convective instability of polymerization. *J. Eng. Math*, 41:13–31, 2001.

J. Edward Anderson. *Magnetohydrodynamic Shock Waves*. The M.I.T. Press, Cambridge, Massachusetts, 1963.

O. G. Benvenuto, J. E. Horvath, and H. Vucetich. Strange-Pulsar Model. *Phys. Rev. Lett.*, 64(7):713–716, 1990.

S. I. Blinnikov, P. V. Sasorov, and S. E. Woosley. Self-Acceleration of Nuclear Flames in Supernovae. *Space Science Reviews*, 74:299–311, November 1995.

Sergei Iv. Blinnikov and Pavel V. Sasorov. Landau-Darrieus instability and the fractal dimension of flame fronts. *Phys. Rev. E*, 53:4827–4841, May 1996.

V. V. Bychkov and M. A. Liberman. Hydrodynamic instabilities of the flame front in white dwarfs. *A&A*, 302:727–734, 1995.

V. V. Bychkov and M. A Liberman. Dynamics and stability of premixed flames. *Physics Reports*, 325: 115–237, 2000.

Fausto Cattaneo. On the Origin of Magnetic Fields in the Quiet Photosphere. *ApJ*, 515:L39–L42, 1999.

S. Chandrasekhar. *Hydrodynamic and Hydromagnetic Stability*. Dover, New York, 1981.

G. Darrieus. Propagation d'un front de flame: Essai de theorie des vitesses anormales de deflagration par développment de la turbulence. *Communication presented at La Technique Moderne*, 1938.

L. J. Dursi, M. Zingale, A. C. Calder, B. Fryxell, F. X. Timmes, N. Vladimirova, R. Rosner, A. Caceres, D. Q. Lamb, K. Olson, P. M. Ricker, K. Riley, A. Siegel, and J. W. Truran. The response of astrophysical thermonuclear flames to curvature and stretch. *ApJ*, 595(2):955–979, October 2003.

M. A. Édel'man. Corrugation Instability of a Strong Slow Parallel Shock Wave. II: Approximate Analytic Investigation. *Astrophysics*, 31:758–764, 1990.

C. S. Gardner and M. D. Kruskal. Stability of Plane Magnetohydrodynamic Shocks. *Phys. Fluids*, 7(5): 700–706, 1964.

Cristian R. Ghezzi, Elisabete M. De Gouveia Dal Pino, and Jorge E. Horvath. Magnetic field effects on the thermonuclear combustion front of chandrasekhar mass white dwarfs. *ApJ*, 548:L193–L196, 2001.

W. Hillebrandt and J. C. Niemeyer. Type Ia Sypernova Explosion Models. *ARA&A*, 38:191–230, 2000.

Patrick Huet, K. Kajantie, Robert G. Leigh, Bao-Hua Liu, and L. McLerran. Hydrodynamic stability analysis of burning bubbles in electroweak theory and QCD. *Phys. Rev. D*, 48(6):2477–2492, September 1993.

K. Kajantie. Hydrodynamic stability of burning QCD walls. *Nuclear Physics A*, 566:551–554, January 1994.

L. Landau. On the slow propagation of burning fronts. *Acta Physiochim. U.R.S.S.*, 77, 1944.

S. Lesin, A. Baron, H. Branover, and J. C. Merchuck. Experimental studies of direct-contact boiling at the superheat limit. *High Temperature*, 31:866–884, 1993.

M. Lesson and N. V. Deshpande. Stability of Magnetohydrodynamic Shock Waves. *Plasma Phys.*, 1(4): 463–472, 1967.

S. A. Markovskii and S. L. Skorokhodov. Oscillatory disintegration of a trans-Alfvénic shock: A magnetohydrodynamic simulation. *Phys. of Plasmas*, 75(1):158–165, January 2000.

S. A. Markovskii and B. V. Somov. Magnetohydrodynamic discontinuties in space plasmas: interrelation between stability and structure. *Space Science Reviews*, 78, 1996.

G. H. Markstein. *Nonsteady Flame Propagation*. Pergamon Press, New York, 1964.

M. Matalon and B. J. Matkowsky. Flames as Gasdynamic Discontinuities. *J. Fluid Mech.*, 124:239–259, 1982.

Yukio Mizutani, Manabu Fuchihata, and Yoshimasa Ohkura. Pre-mixed laminar flames in a uniform magnetic field. *Combustion and Flame*, 125:1071–1073, 2001.

Pierre Pelce and Paul Clavin. Influience of hydrodynamics and diffusion upon the stability limits of laminar premixed flames. *J. Fluid Mech.*, 124:219–237, 1982.

A. R. Piriz and R. F. Portugues. Landau-Darrieus instability in an ablation front. *Phys. Plasmas*, 10(6): 2449–2456, 2003.

N. V. Pogorelov and T. Matsuda. Nonevolutionary MHD shocks in the solar wind and interstellar medium interaction. *A&A*, 354:697–702, 2000.

Ravi Samtaney. Suppression of the Richtmyer-Meshkov instability in the presence of a magnetic field. *Phys. of Fluids*, 15(8):L53–L56, August 2003.

Gary D. Schmidt, Hugh C. Harris, James Lievert, Daniel J. Eisenstein, Scott F. Anderson, J. Brinkmann, Patrick B. Hall, Michael Harvanek, Suzanne Hawley, S. J. Kleinman, Gillian R. Knapp, Jurek Krzesinski, Don Q. Lamb, Dan Long, Jeffrey A. Munn, Eric H. Neilsen, Peter R. Newman, Atsuko Nitta, David J. Schlegel, Donald P. Schneider, Nicole M. Silvestri, J. Allyn Smith, Sephanie A. Snedden, Paula Skody, and Dan Vanden Verk. Magnetic White Dwarfs from the SDSS. The First Data Release. *ApJ*, 595(2):1101–1113, October 2003.

Frank H. Shu. *The Physics Of Astrophysics, Volume II: Gas Dynamics*. Univeristy Science Books, Mill Valley, CA, 1992.

James M. Stone and Mark Edelman. The corrugation instability in slow magnetosonic shock waves. *ApJ*, 454:182–193, 1995.

D. A. Tidman and N. A. Krall. *Shock Waves in Collisionless Plasmas*. Wiley, New York, 1971.

F. X. Timmes and S. E. Woosley. The conductive propagation of nuclear flames. I - Degenerate C + O and O + Ne + Mg white dwarfs. *ApJ*, 396:649–667, September 1992.

Nobuko I. Wakayama and Masaaki Sugie. Magnetic promotion of combustion in diffusion flames. *Physica B*, 216:403–405, 1996.

D. T. Wickramasinghe and Lilia Ferrario. Magnetism in isolated and binary white dwarfs. *PASP*, 112: 873–924, 2000.

F. A. Williams. *Combustion Theory*. Benjamin/Cummings Publishing Company, Menlo Park, California, 2nd edition, 1985.

Ya. B. Zeldovich and D. A. Frank-Kamenetskii. The theory of thermal propagation of flame. *Zh. Fiz. Khim*, 12:100, 1938.

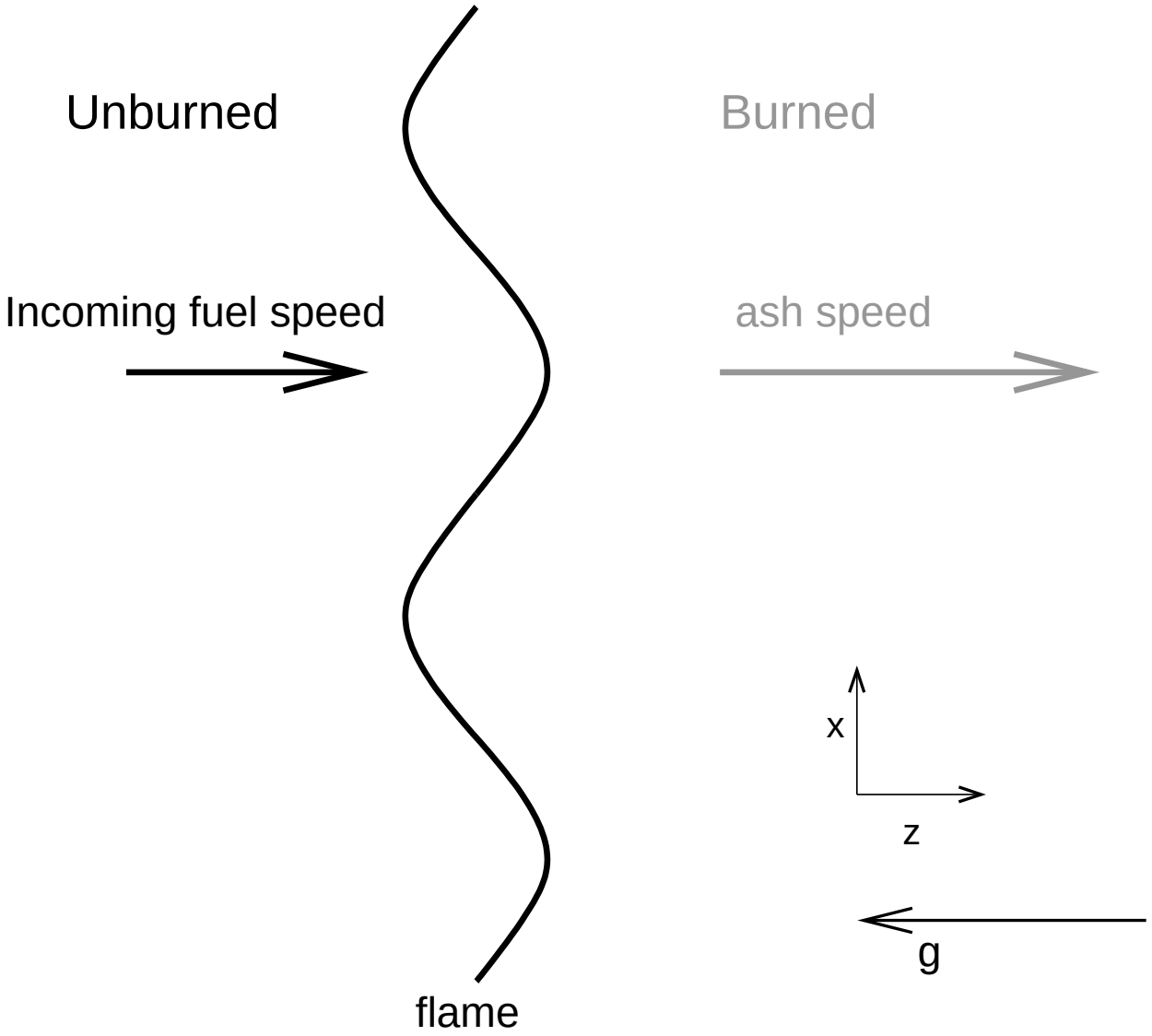

Fig. 1.— A sketch of the physical setup of the Landau-Darrieus instability in the frame of the flame front.

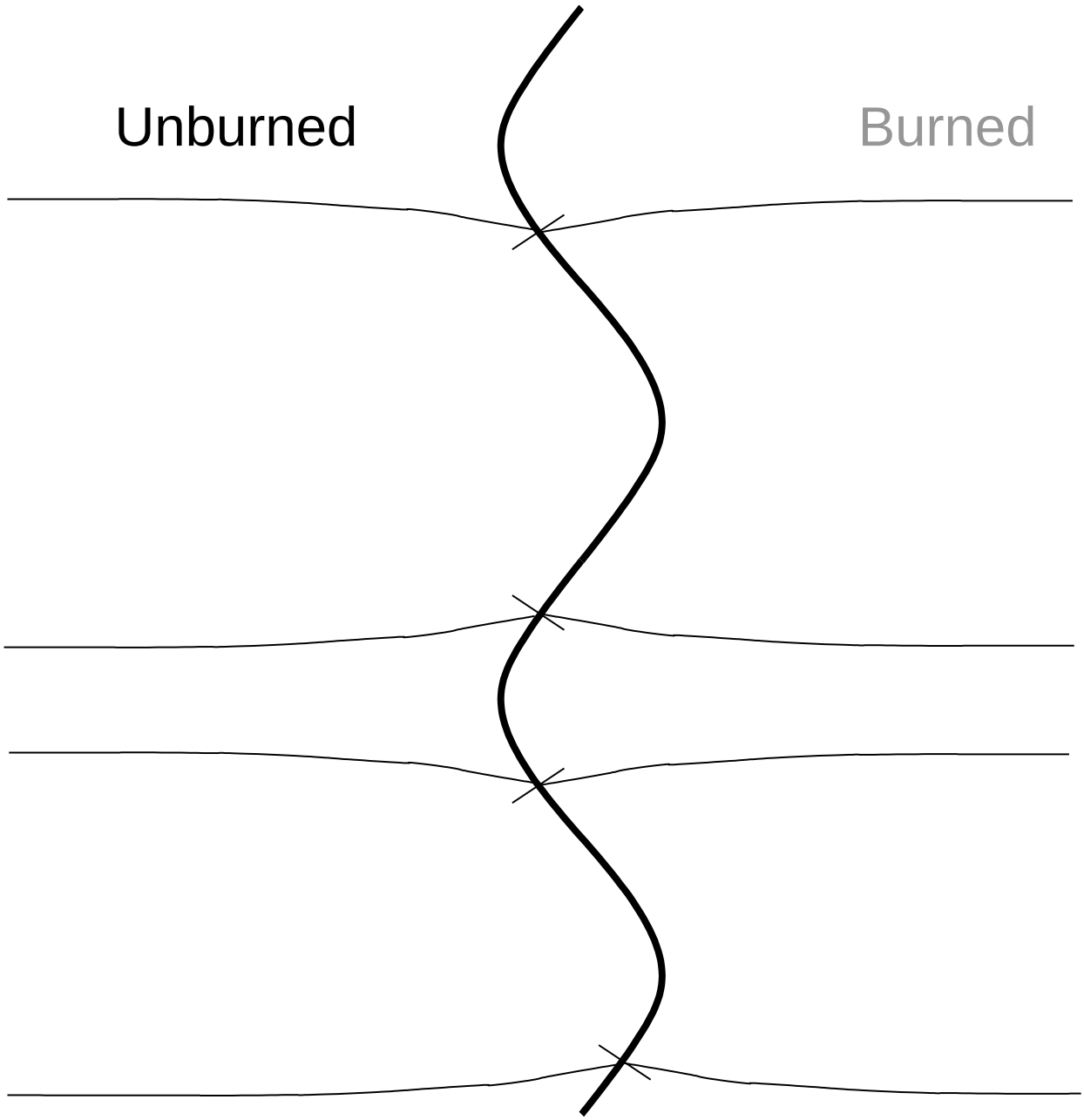

Fig. 2.— Because the tangential component of velocity is constant across the flame in the hydrodynamical case, while the normal component jumps, streamlines crossing the flame are bent towards the flame normal. Since at large distances the streamlines must remain parallel, the stream lines 'fan out' near flame surfaces curved towards the unburned gas; this locally reduces the flow velocity, allowing the flame in that region to propagate further ahead. (Figure taken after Williams (1985) Fig. 9.8).

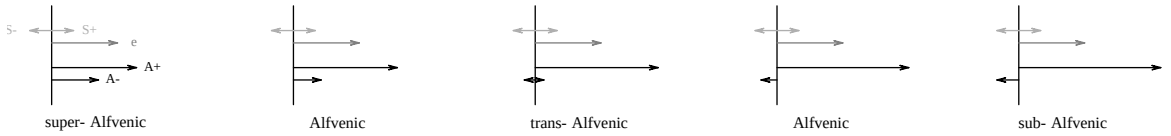

Fig. 3.— The waves and their speeds propagating from the flame (vertical line), following Anderson (1963), in the case of the field parallel to flame propagation. The waves shown, top to bottom, are $C^{(s^-)}/C^{(s^+)}$, $C^{(e)}$, $C^{(A^+)}$, and $C^{(A^-)}$. From left to right, the states are: super-Alfvénic ($\bar{a}_u < 1$); 'switch on' Alfvénic, ($\bar{a}_u = 1$); trans-Alfvénic ($1 < \bar{a}_u < \sqrt{\alpha}$); 'switch off' Alfvénic, ($\bar{a}_u = \sqrt{\alpha}$); and sub-Alfvénic ($\bar{a}_u > \sqrt{\alpha}$).

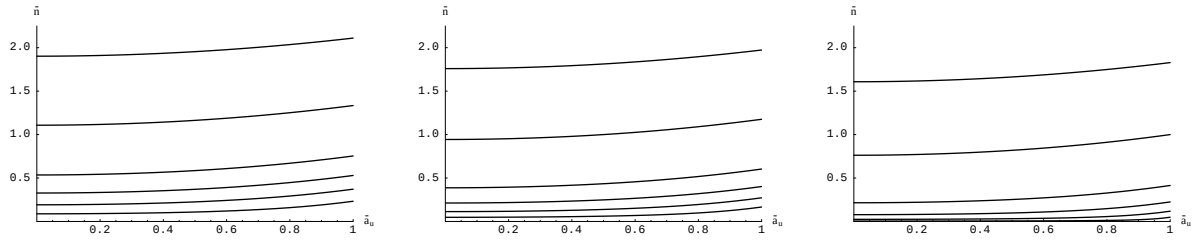

Fig. 4.— The growth rate for a parallel magnetic field when the flame is everywhere super-Alfvénic. We plot the maximum real part of the scaled growth rate ($\bar{n}$) as a function of $\bar{a}_u$, with $\bar{g} = -1$ (destabilizing) on the left, $\bar{g} = 0$ in the center, and $\bar{g} = +1$ (stabilizing) on the right. Lines are plotted for, top to bottom, $\alpha = 8$, 4, 2, 1.5, 1.25, 1.1.

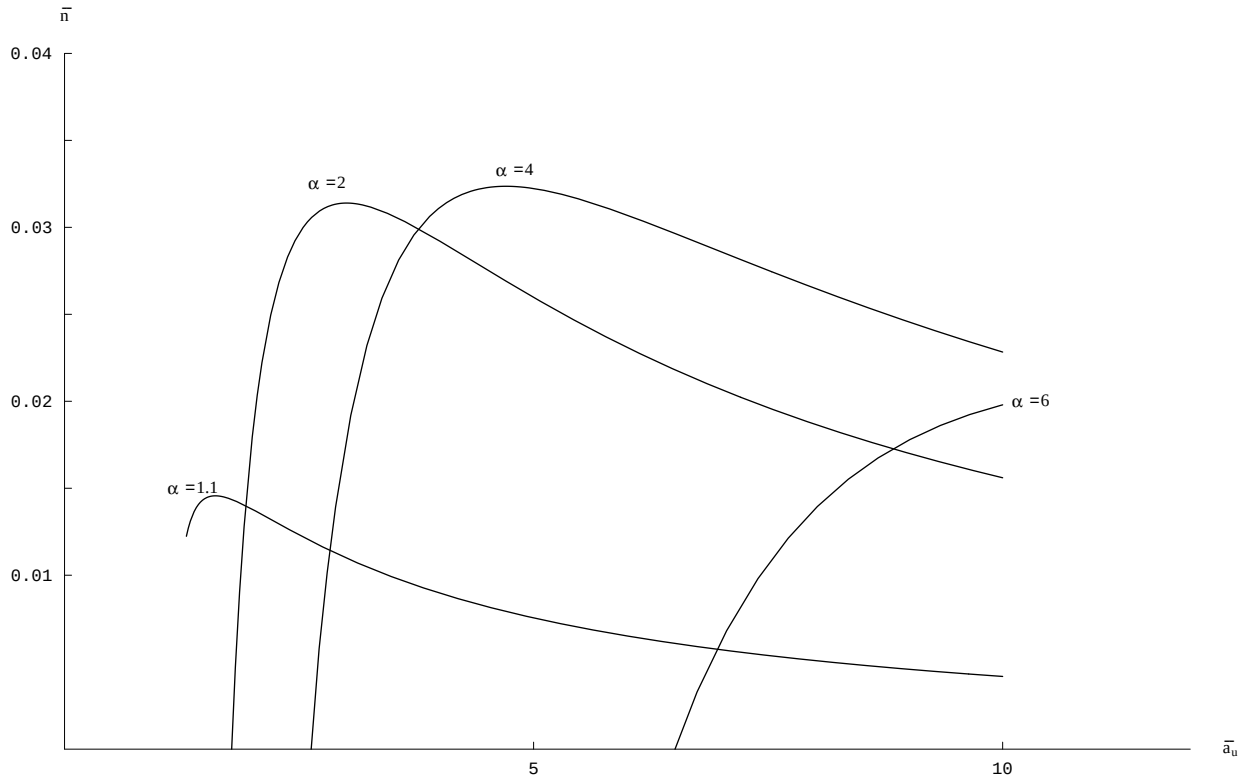

Fig. 5.— The growth rate for a parallel magnetic field in the sub-Alfvénic case with destabilizing gravity; with zero or stabilizing gravity, the flame is stable. We plot the maximum real part of the scaled growth rate ($\bar{n}$) as a function of $\bar{a}_u$, with $\bar{g} = -1$. Lines are plotted for, left to right, $\alpha = 1.1$, 2, 4, 6.

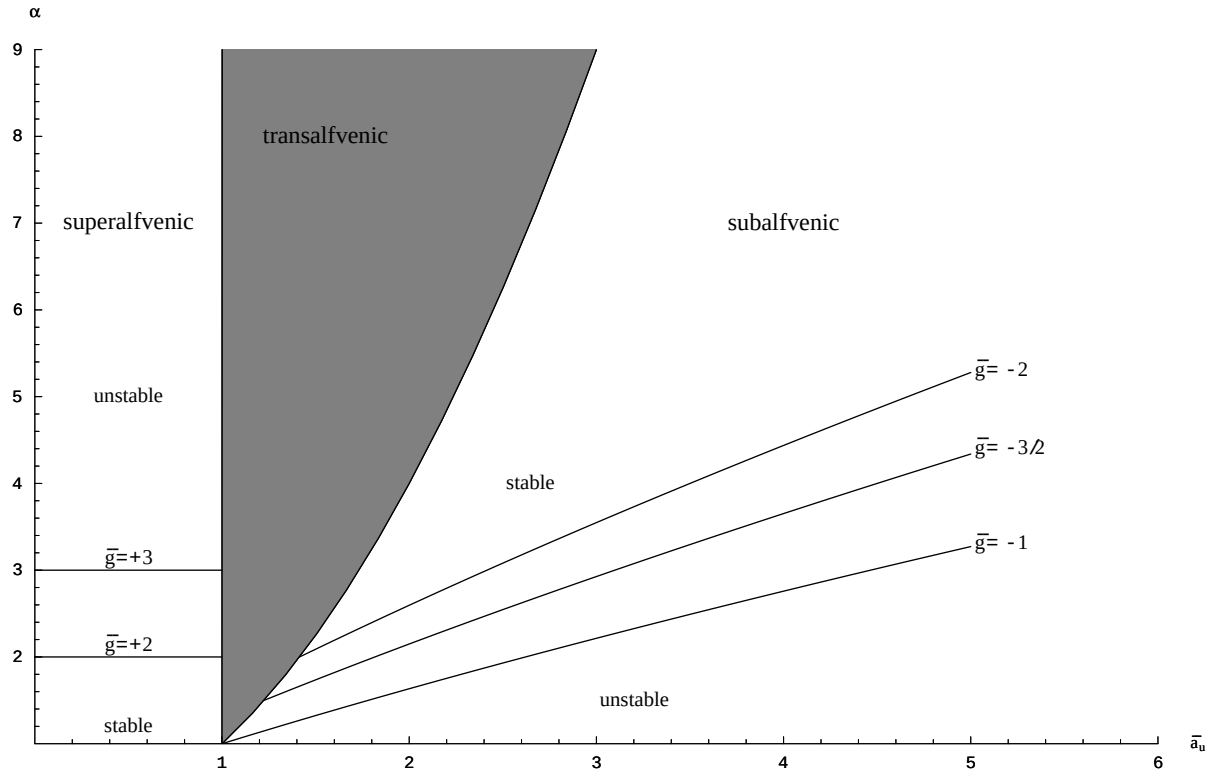

Fig. 6.— Stability boundaries in α for the case of a parallel magnetic field as a function of $\bar{a}_u$. Note that for the superalfvénic case, the region above the curves is unstable, and for the subalfvénic case, the region below the curves is unstable.

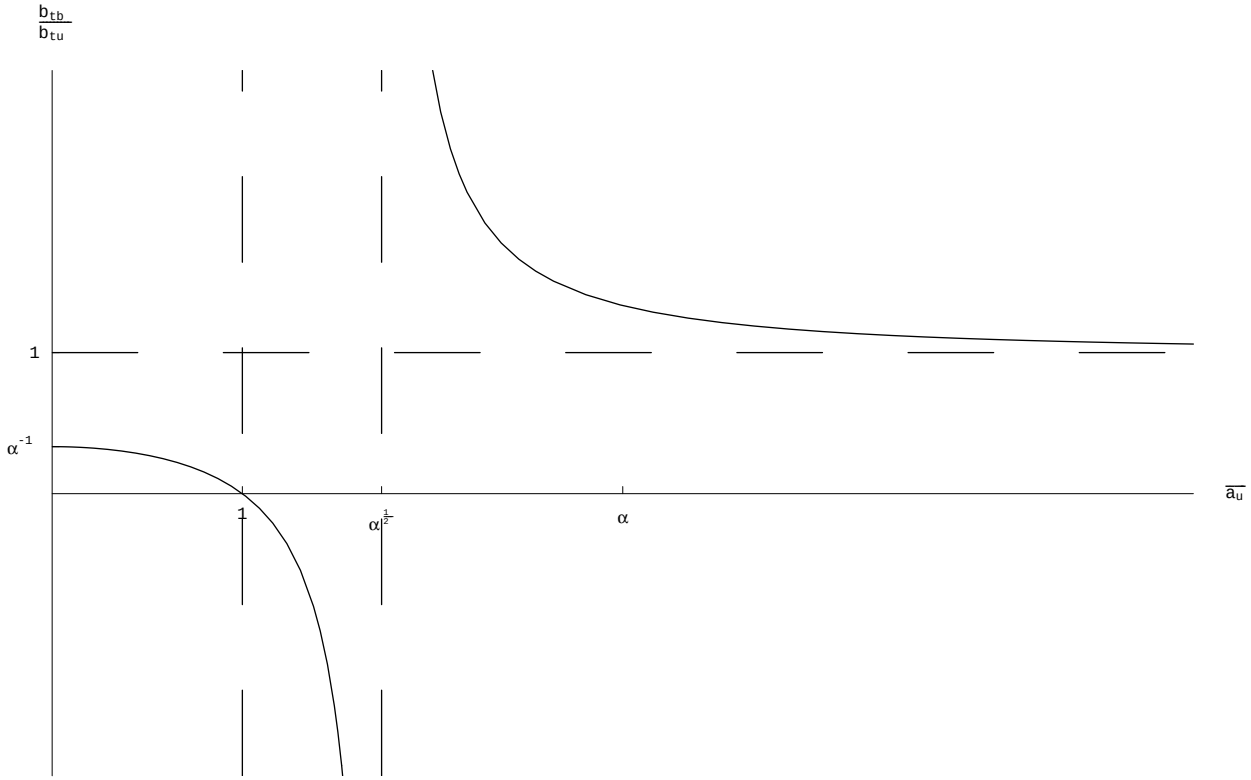

Fig. 7.— Plotted is the ratio of the tangential magnetic field at the interface in the burned fluid to that in the fuel, $B_{tb}/B_{tu} = ([B_t]/B_{tu}) + 1$. At $\bar{a}_u = 1$, the flame is a 'switch off' discontinuity; at $\bar{a}_u = \sqrt{\alpha}$, the flame is a 'switch on' discontinuity.

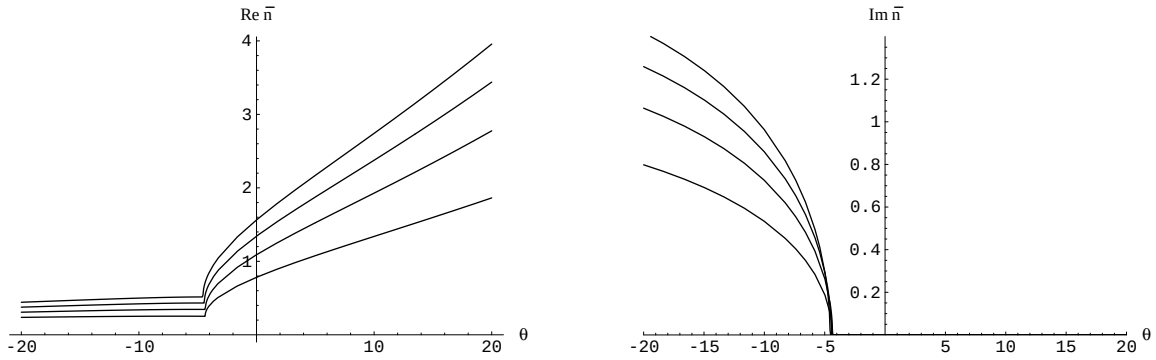

Fig. 8.— On the left, the maximum real part of the scaled growth rate ($\bar{n}$) in the trans-Alfvénic case, with $\bar{g} = 0$, $\bar{a}_u = 1.3$, and α (top to bottom) 5,4,3,2. On the right, the corresponding imaginary component. For any value of θ the flame is unstable; the flame can only partially stabilize itself by sending forward fairly strong (several times the amplitude of the $C^{(s-)}$ wave) and oscillatory Alfvén waves.

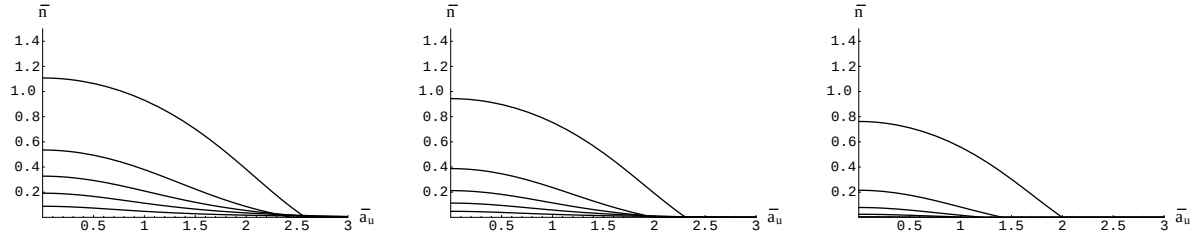

Fig. 9.— The maximum real part of the scaled growth rate ($\bar{n}$) for the case of a perpendicular magnetic field as a function of $\bar{a}_u$, with $\bar{g} = -1$ on the left, $\bar{g} = 0$ in the center, and $\bar{g} = +1$ on the right. Lines are plotted for, top to bottom, $\alpha = 4$, 2, 1.5, 1.25, and 1.1

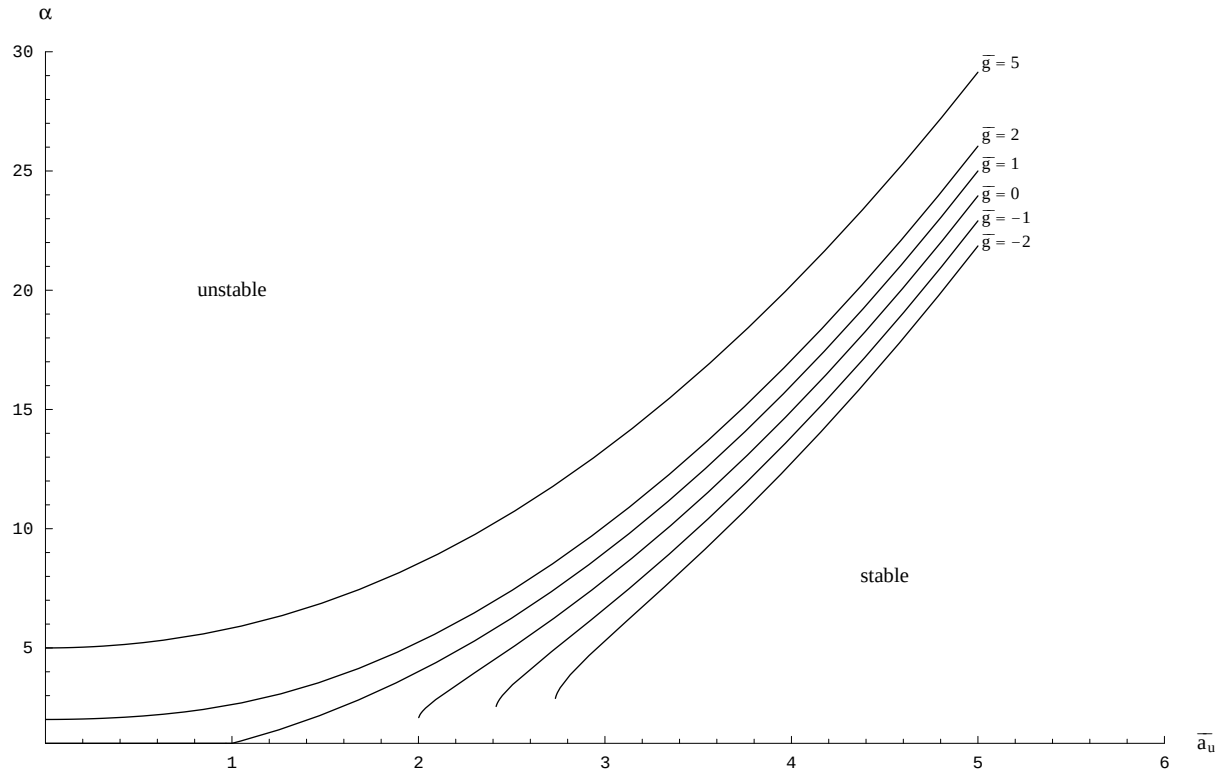

Fig. 10.— Stability boundaries in α for the case of a perpendicular magnetic field as a function of $\bar{a}_u$, for (top to bottom) $\bar{g}$ = 5,2,1,0,-1,-2.

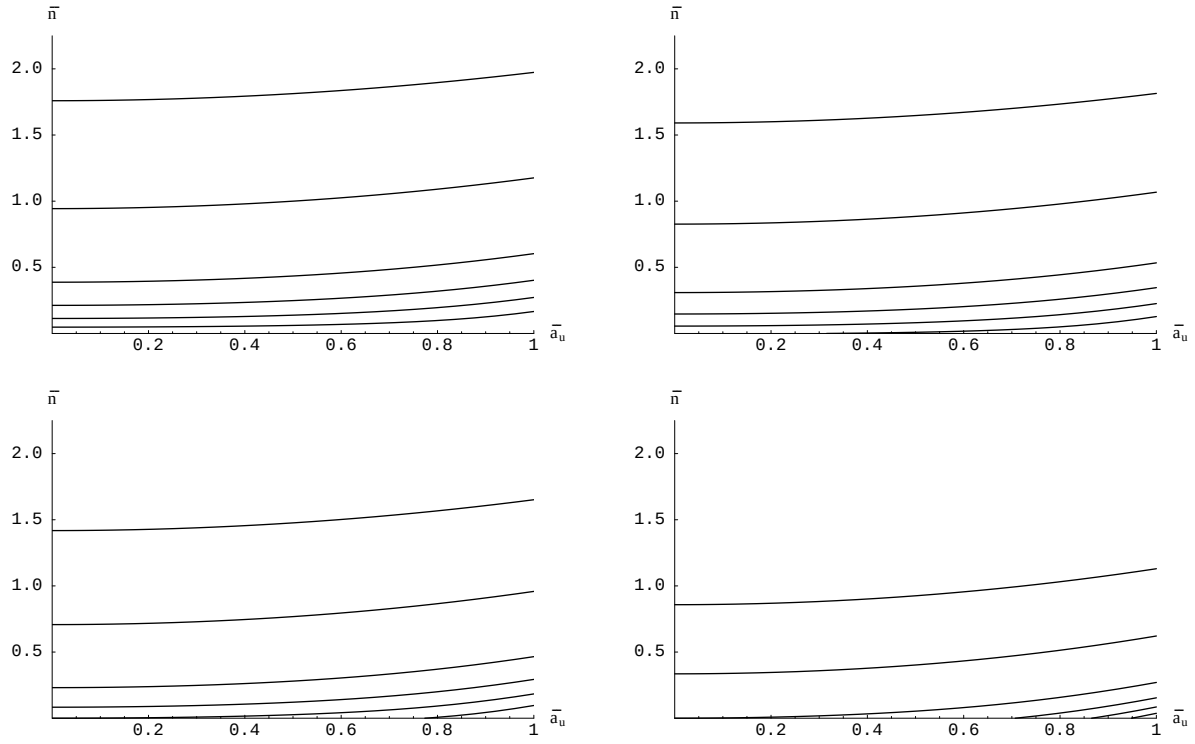

Fig. 11.— The growth rate for a parallel magnetic field when the flame is everywhere super-Alfvénic, and has a negative Markstein length. We plot the maximum real part of the scaled growth rate ($\bar{n}$) as a function of $\bar{a}_u$, with $\bar{l}_M = 0$ on the top left, $\bar{l}_M = -0.05$ on top right, $\bar{l}_M = -0.10$ on the bottom left, and $\bar{l}_M = -0.25$ on the bottom right. Lines are plotted for, top to bottom, $\alpha = 8$, 4, 2, 1.5, 1.25, 1.1.